

In-plane magnetic properties of as-spun $Y_xPr_{1-x}Co_5$ ribbons ($x = 0.25, 0.50, 0.75$)

A. Santana Gil^a, J.L. Sanchez Ll^{a,c,*}, R. Valenzuela^b, B. Hernando^c, M.J. Pérez^c, J.D. Santos^c

^aLaboratorio de Magnetismo, Facultad de Física-IMRE, Universidad de La Habana, La Habana 10400, Cuba

^bInstituto de Investigaciones en Materiales, Universidad Nacional Autónoma de México, P.O. Box 70-360, Coyoacán, México D.F., 04510, México

^cDepartamento de Física, Facultad de Ciencias, Universidad de Oviedo, Calvo Sotelo s/n, 33007 Oviedo, Spain

Available online 28 February 2007

Abstract

As-spun ribbons of $Y_xPr_{1-x}Co_5$ alloys with $x = 0.25, 0.50$, and 0.75 , were produced by single-roller melt spinning at wheel speeds of 5, 15, and 40 ms^{-1} . X-ray diffraction patterns and SEM micrographs show that samples are essentially single phase with the hexagonal $CaCu_5$ -type crystal structure and dendritic microstructure. Hysteresis loops were measured in the plane of ribbons applying the magnetic field along and perpendicular to ribbon plane. Samples exhibit in-plane reduced remanence above 0.5, with a noticeable value of 0.86 for the alloy $Y_{0.5}Pr_{0.5}Co_5$ quenched at $v = 15\text{ ms}^{-1}$. XRD patterns obtained for the surface of ribbons confirmed that the high remanence measured results from the preferential orientation of 1:5 grains with their c -axis parallel to the ribbon plane. This in-plane crystallographic texture is attributed to the directional solidification induced by thermal gradient during rapid quenching. Coercivity rises with the increase of both, Pr content and wheel speed with values in the range 1.0–5.2 kOe.

© 2007 Elsevier B.V. All rights reserved.

PACS: 74.25.Ha; 75.50.Vv; 73.63.Bd; 75.50.Ww

Keywords: Permanent magnet; Magnetic properties; Magnetic anisotropy; High-coercivity materials

1. Introduction

YCo_5 and $PrCo_5$ compounds combine saturation induction and Curie points similar to those of $SmCo_5$ with a large uniaxial anisotropy field to produce high intrinsic coercivity, iH_C , being excellent candidates for the development of permanent magnets with a high maximum energy product $(BH)_{\max}$ [1,2]. However, magnets based on these compounds have not been commercialized due to the technical difficulties found to develop high enough and well-reproducible coercivity values in powdered or sintered alloys [3,4]. A microstructural refinement by rapid quenching has been attempted to overcome this problem. In as-spun alloys obtained by single-roller melt spinning at a high wheel speed, the 1:5 phase forms from the melt but owing to the fast grain growth kinetic micrometric grains with relatively low coercivities are obtained [5–7]. How-

ever, in rapidly quenched ribbons of YCo_5 obtained at a medium wheel surface speed, v , of 25 ms^{-1} , a significant crystallographic texture, with a preference for the c -axis of 1:5 crystallites along the plane of ribbons, was reported [7]; a similar behavior was previously observed for the isostructural $CaCu_5$ -type hexagonal compounds $SmCo_5$ [8], $(Sm,Gd)Co_5$ [9], and $Sm(Co,Cu)_5$ [10] quenched at low wheel speed ($v = 5\text{--}6\text{ ms}^{-1}$). Since texture is a key precondition to achieve high $(BH)_{\max}$ we investigated on the phase constitution, microstructure, and in-plane room-temperature magnetic properties of ternary as-spun $Y_xPr_{1-x}Co_5$ alloys with the intermediate compositions $x = 0.25, 0.50$, and 0.75 , processed at wheel speeds of 5, 15, and 40 ms^{-1} . The most significant results are presented in this report.

2. Experimental

Ingots of 3 gm with nominal composition $Y_xPr_{1-x}Co_5$ and $x = 0.25, 0.50$, and 0.75 , were produced by arc melting

*Corresponding author. Tel.: +5378788958x227; fax: +5378734869.
E-mail address: sanchez@nanomagnetism.org (J.L. Sanchez Ll).

under an Ar highly pure atmosphere. A home-made melt spinner with a copper wheel of 20 cm in diameter was employed to obtain melt spun ribbons in a helium environment. Master alloys were inserted into quartz tubes with an inner diameter of 1.8 cm and circular nozzle of ~ 0.8 mm. Molten alloys were ejected applying a controlled helium overpressure on the surface of the wheel rotating at linear speeds of 5, 15, and 40 ms^{-1} , respectively. Hereafter, the free surface of ribbons will be referred as ‘non-contact surface’.

X-ray diffraction (XRD) patterns were obtained in a high-resolution Seifert model 3000 TT diffractometer with $\text{Cu-K}\alpha$ radiation. Fragments of ribbons, of approximately 0.25–0.5 cm in length and a thickness of 10–30 μm (dependent on wheel speed), were placed one parallel to each other to cover as possible the sample holder area. Scanning electron micrographs were taken for both, contact and non-contact surface side of ribbons using a JEOL model JSM-6100 scanning electron microscope. Hysteresis loops were recorded at room temperature in a vibrating sample magnetometer LDJ model 9600 with a maximum saturation field of $H_{\text{max}} = 16 \text{ kOe}$.

3. Results and discussion

XRD patterns of powdered arc-melted $\text{Y}_x\text{Pr}_{1-x}\text{Co}_5$ buttons indicated that starting master alloys were in effect single phase with the hexagonal CaCu_5 -type crystal structure in the whole composition range. The relative intensity of the peaks is in agreement with that reported for randomly oriented 1:5 crystalline grains [10]. A representative indexed pattern is plotted in Fig. 1(a). It is compared with that of as-spun ribbons having the same nominal composition where the non-contact surface of ribbon was exposed to XRD radiation (Fig. 1(b)).

The main diffraction peaks belong to the 1:5 structure but a notable change in the relative intensity of some main lines is observed. In fact, the relative intensity of (200) and (110) reflections is considerably stronger than that of the isotropic sample, while that of (101) and (111) is much weaker, indicating that c -axes of crystallites preferentially align along ribbon plane. A Rietveld refinement of both patterns based on the hexagonal CaCu_5 -type structure led to the following lattice parameters: (a) arc-melted alloy: $a = 4.980 \text{ \AA}$ and $c = 3.983 \text{ \AA}$; as-spun ribbons: $a = 4.97215 \text{ \AA}$ and $c = 3.53223 \text{ \AA}$. Also note the presence of two minor broad XRD peaks at $2\theta \cong 29.57^\circ$ and 44.05° that were identified as $(\text{Y,Pr})_2\text{O}_3$ indicating a certain surface oxidation. A similar texture effect was observed for all the samples obtained. The effect was not very dependent of which surface of the ribbons is exposed to XRD radiation.

Fig. 2 shows SEM pictures of the non-contact surface of ribbons with $x = 0.5$ quenched at $v = 15 \text{ ms}^{-1}$. All the alloys studied show a similar microstructure that consisted of micronic dendrites, of about 1–9 μm in length, with the long axis parallel to ribbon plane. In agreement with XRD

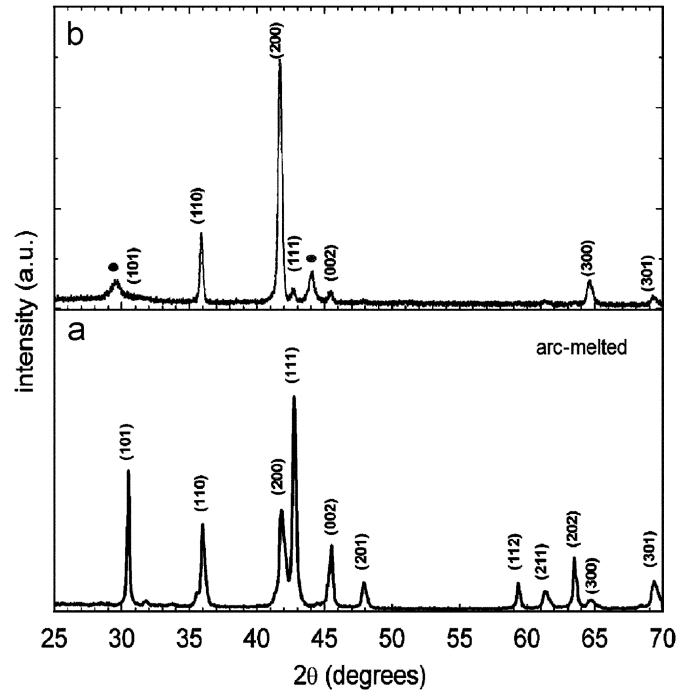


Fig. 1. X-ray diffraction pattern for $\text{Y}_{0.5}\text{Pr}_{0.5}\text{Co}_5$ alloys: (a) arc-melted powdered master alloy and (b) as-spun ribbons obtained at $v = 15 \text{ ms}^{-1}$; the non-contact surface of ribbons was exposed to XRD radiation.

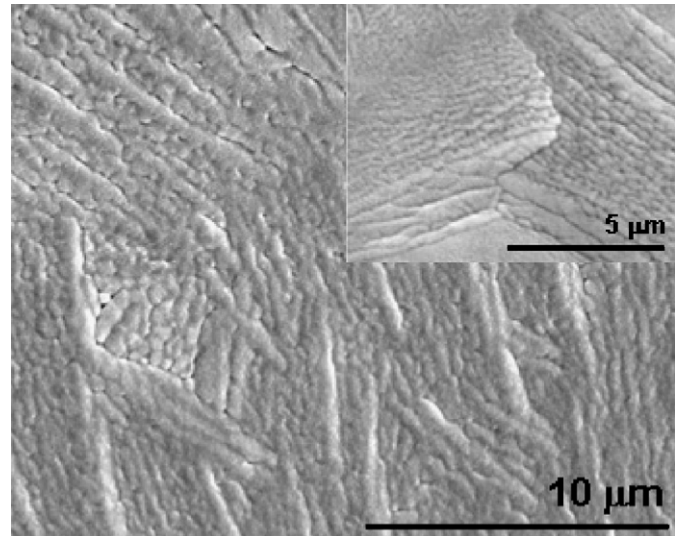


Fig. 2. SEM micrographs at different magnifications of the non-contact ribbon surface for as-spun $\text{Y}_{0.5}\text{Pr}_{0.5}\text{Co}_5$ samples.

data are suggested that the c -axis of 1:5 grains and the dendritic growing direction is coincident; a similar microstructure was obtained for YCo_5 [7]. For the surface in contact with the wheel a finer and less dendritic-like microstructure was systematically observed in accordance with the higher solidification rate.

Representative hysteresis loops, recorded with the magnetic field applied parallel and perpendicular to ribbon plane, are plotted in Fig. 3. Their differences in saturation magnetization and coercivity are in agreement with the in-

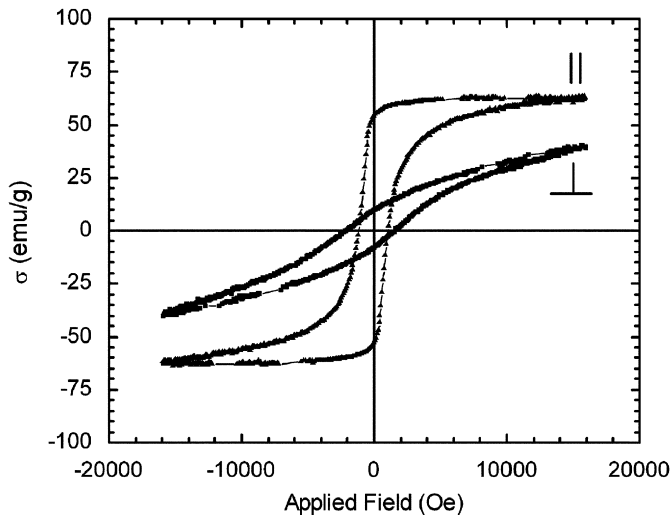


Fig. 3. Hysteresis loops for as-spun $Y_{0.5}Pr_{0.5}Co_5$ ribbon quenched at $v = 15 \text{ ms}^{-1}$, applying the magnetic field parallel and perpendicular to ribbon plane.

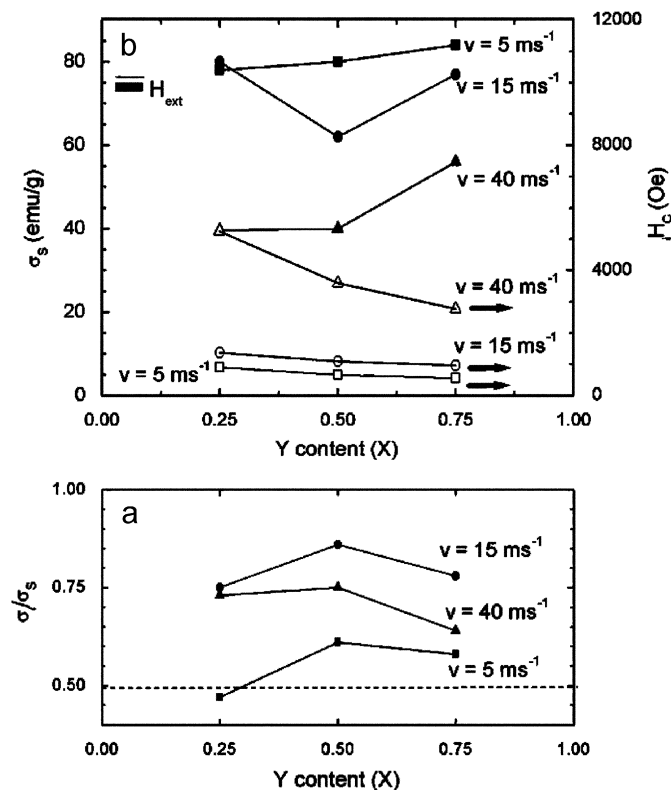


Fig. 4. Magnetic properties measured along ribbon length for as-spun $Y_xPr_{1-x}Co_5$ alloys: (a) reduced remanence σ_r/σ_s and (b) saturation magnetization and coercivity (closed and open symbols, respectively).

plane crystallographic texture effect revealed by XRD where the c -axis of the 1:5 phase is aligned along ribbon plane. The dependence of magnetic properties on Yttrium content and quenching rate measured along ribbon plane is reported in Fig. 4. Fig. 4(a) clearly shows that, except for the alloy $Y_{0.25}Pr_{0.75}Co_5$ quenched at $v = 5 \text{ ms}^{-1}$, the

reduced remanence, σ_r/σ_s , is systematically over the predicted value of 0.5 for randomly oriented single-domain grains with uniaxial anisotropy in the remnant state [2]. The highest values were achieved for alloys quenched at $v = 15 \text{ ms}^{-1}$ with a maximum of 0.86 for $x = 0.5$. Specific saturation magnetization, σ_s , and intrinsic coercive fields, iH_C , are in agreement with those previously reported for RCo_5 ($R = Y, Pr$) ribbons [5–7]. The coercivity increases with the increasing in both Pr content and wheel speed. The highest iH_C value, 5.2 kOe, was obtained for $x = 0.25$ and $v = 40 \text{ ms}^{-1}$.

4. Conclusions

Rapidly solidified ribbons with nominal composition $Y_xPr_{1-x}Co_5$ ($x = 0.25, 0.50, \text{ and } 0.75$), obtained at wheel speeds of 5, 15, and 40 ms^{-1} were characterized by X-ray diffraction, scanning electron microscopy, and magnetic measurements. Ribbons, that are nearly single phase with the $CaCu_5$ -type crystal structure, crystallize in a dendritic microstructure exhibiting a remarkable crystallographic and magnetic texture along the ribbon plane. However, in agreement with previous works, the insufficient coercivity attained is still the main limitation for the fabrication of permanent magnets based on these alloys. Further studies are in course in order to understand better the role of the different synthesis conditions on texture and coercivity to optimize these relevant technical properties.

Acknowledgments

A. Santana Gil acknowledges the support received from “Red de Macro Universidades de America Latina y El Caribe” for visiting IIM-UNAM (Grant no. RMU/OBSV/075/05). Present investigation was also financially supported by MEC, Spain (research project MAT2003-06942). Authors are grateful to Dr. R. Guzman (IIM-UNAM) and Dr. A.J. Quintana García for the assistance in SEM observations (Servicios Científico Técnicos, University of Oviedo). J.L. Sánchez LI is grateful to University of Oviedo for making possible his stay at this center.

References

- [1] K.J. Strnat, in: E.P. Wohlfarth, K.H.J. Buschow (Eds.), Ferromagnetic Materials, North-Holland, Amsterdam, vol. 4, 1988, p. 131.
- [2] R. Skomski, J.M.D. Coey, Permanent Magnetism, Studies in Condensed Matter Physics, Institute of Physics Publishing, Bristol and Philadelphia, 1999.
- [3] W.E. Wallace, R.S. Craig, H.O. Gupta, S. Hirosawa, A. Pedziwiatr, E. Oswald, E. Schwab, IEEE Trans. Magn. 20 (1984) 1599.
- [4] E.M.T. Velu, R.T. Obermyer, S.G. Sankar, W.E. Wallace, J. Less-Common Metals 148 (1989) 67.
- [5] C.D. Fuerst, J.F. Herbst, C.B. Murphy, D.J. Van Wingerden, J. Appl. Phys. 74 (1993) 4651.
- [6] J.L. Sánchez LI, A. Santana Gil, R. Bustamante Salazar, B. Hernando, J.D. Santos, M.J. Pérez, H. Salim de Amorim,

- The Physics of Metals and Metallography 99 (Suppl. 1) (2005) S34.
- [7] J.T. Elizalde Galindo, J.A. Matutes Aquino, H.A. Davies, Z. Liu, J. Magn. Magn. Mater. 294 (2005) 137.
- [8] J. Ding, P.G. McCormick, R. Street, J. Alloys Compds. 228 (1995) 102.
- [9] W.-Y. Zhang, B.-G. Shen, Z.-H. Cheng, L. Li, Y.-Q. Zhou, J.-Q. Li, Appl. Phys. Lett. 79 (2001) 1843.
- [10] A.-R. Yan, W.-Y. Zhang, H.-W. Zhang, B.-G. Shen, J. Appl. Phys. 88 (2000) 2787.